

RXTE/HEXTE Analysis of the Crab Pulsar Glitch of July 2000

M. Vivekanand¹

(Accepted for publication by ApJ on 28 Mar 2015)

ABSTRACT

Hard xray data from the RXTE observatory (HEXTE energy range 15 to 240 keV) have been analyzed to obtain a phase coherent timing solution for the Crab pulsar glitch of 15 July 2000. The results are: (1) step change in the rotation frequency ν_0 of the Crab pulsar at the epoch of the glitch is $\Delta\nu_0 = (30 \pm 3) \times 10^{-9} \times \nu_0$, (2) step change in its time derivative is $\Delta\dot{\nu}_0 = (4.8 \pm 0.6) \times 10^{-3} \times \dot{\nu}_0$, and (3) the time scale of decay of the the step change is $\tau_d = 4.7 \pm 0.5$ days. The first two results are consistent with those obtained at radio frequencies by the Jodrell Bank observatory. The last result has not been quoted in the literature, but could be an underestimate due to lack of observations very close to the glitch epoch. By comparing with the monthly timing ephemeris published by the Jodrell group for the Crab pulsar, the time delay between the main peaks of the hard xray and radio pulse profiles is estimated to be $+411 \pm 167 \mu\text{sec}$. Although this number is not very significant, it is consistent with the number derived for the 2 to 16 keV energy range, using the PCA instrument of RXTE. The separation between the two peaks of the integrated pulse profile of the Crab pulsar, and the ratio of their intensities, both are statistically similar before and after the glitch. The dead time corrected integrated photon flux within the integrated pulse profile appears to decrease after the glitch, although this is not a statistically strong result. This work achieves what can be considered to be almost absolute timing analysis of the Crab pulsar hard xray data.

Subject headings: pulsars: individual (Crab Pulsar) X-rays: stars

1. Introduction

Glitches in pulsars are events in which the rotation period and its derivative (and possibly higher derivatives as well) undergo an abrupt change in value, on time scales of less than minutes, often followed by a recovery to approximately the pre glitch values, over time scales of days to tens of days, or even much longer; see (Shemar & Lyne 1996; Lyne et al. 2000; Wong et al. 2001; Espinoza et al. 2011) for details of pulsar glitches, their history and their relevance. Glitches are important to study because they are probably one of the very few methods available to study the internal structure of neutron stars (Baym et al. 1969); see also

(Ruderman et al. 1998) and references therein. Glitches are rare events; in the Crab pulsar (PSR B0531+21 or J0534+2200) they occur once in ≈ 1.6 years (Espinoza et al. 2011). A typical glitch in the Crab pulsar involves a very small fractional change of rotation period (or alternately, rotation frequency) of about 10^{-7} to 10^{-9} (Wong et al. 2001; Espinoza et al. 2011). Coupled with the sudden onset of a glitch, this implies that frequent and regular pulsar timing observations are required to study the glitch phenomenon. The very low rotation period of the Crab pulsar ($P \approx 33.5$ ms, or alternately very high rotation frequency $\nu \approx 29.851$ Hz, at the middle of the year 2000) necessitates timing observations at least twice a day, over a period of one year, to properly analyze a glitch; see (Manchester & Taylor 1977; Backer & Hellings 1986; Lyne & Smith 2006) for pedagogical reviews of pulsar timing in general, and analysis of pulsar glitches in particular.

¹No. 24, NTI Layout 1st Stage, 3rd Main, 1st Cross, Nagasettyhalli, Bangalore 560094, India. (viv.maddali@gmail.com)

Clearly a dedicated telescope is required to study pulsar glitches. At radio frequencies this has been done (and continues to be done) for the Crab pulsar by the Jodrell Bank observatory (Lyne et al. 1993). Over the last ≈ 40 years, they have accumulated pulse timing information of the Crab pulsar at 610 and 1400 MHz radio frequencies, observing it daily, and have published (and continue to update) the monthly timing ephemeris¹ of the Crab pulsar; see (Lyne et al. 1993) for details; also see (Lyne et al. 2015) for the 45 year rotation history of the Crab pulsar. The Crab pulsar has also been observed daily by the Green Bank Telescope, at 327 and 610 MHz radio frequencies (Backer et al. 2000; Wong et al. 2001). Ideally such work should have been carried out at xray energies, which are not affected by problems associated with propagation through the interstellar medium, that radio signals are susceptible to (Lyne et al. 1993; Backer et al. 2000). However, xray telescopes are difficult to build and expensive, in comparison to radio telescopes. RXTE is one of the few xray observatories that can time the arrival of pulses from pulsars to the accuracy required for timing analysis. However RXTE is not a dedicated pulsar timing observatory, and most Crab pulsar observations of RXTE are spaced, on the average, two weeks apart. Fortunately, during the period late 1999 to late 2000, three sets of very closely spaced RXTE observations of the Crab pulsar were available, one of them being just after glitch of 15 July 2000. It is mainly these three clusters of observations, and the existence of observations immediately after the glitch, that have motivated this work.

This work is organized as follows. Section 2 and section 3 describe HEXTE data and the method of analysis. Section 4 presents phase coherent timing results for the July 2000 glitch of the Crab pulsar. Section 5 contains discussion and describes the behavior of some Crab pulsar parameters before and after the glitch.

2. Observations

The HEXTE instrument (Rothschild et al. 1998) of RXTE consists of two independent clusters of detectors, labeled clusters 0 and 1. Each cluster contains four NaI(Tl)/CsI(Na) phoswich

scintillation photon counters, and has a field of view of one degree in the sky. For practical purposes this instrument is sensitive to photons in the 15 to 240 keV range, and each photon’s arrival time is measured with an accuracy of $\approx 7.6 \mu\text{sec}$ (see “The ABC of XTE” guide on the RXTE website²). During normal operation, the two clusters switch between the source and a background region of the sky, such that when one cluster is pointed at the source, the other is pointed at the background, and vice versa. For pulsar observations another mode of observation is also used, in which both clusters dwell only on the source. The data used in this work consist of both modes, but predominantly of the latter kind.

The first observation used in this work was obtained on 18 Dec 1999, and the last on 24 Dec 2000; the corresponding observation identification numbers (ObsID) for the data are 40090-01-01-00 and 50804-01-14-00, respectively. The epoch of the glitch is $\text{MJD } 51740.656 \pm 0.002$ (Espinoza et al. 2011), which is at $\approx 15:45$ UTC on 15 July 2000. The pre glitch data is relatively more frequently observed during the months Dec 1999 and Jan 2000, but not later. It extends up to 14 May 2000 only (ObsID 50099-01-26-00), which implies that no observations exist for the two month duration just prior to the glitch. Fortunately, the first post glitch observation is on 17 July 2000 at $\approx 00:45$ UTC (ObsID 50098-01-01-00), which is just ≈ 1.4 days after the glitch. From then onward the data is well sampled (frequently observed) up to 31 Jul 2000 (ObsID 50099-01-02-00), after which the data is under sampled until 5 Dec 2000 (ObsID 50099-01-11-00), which is for most of the post glitch duration. Then again the data is well sampled until 24 Dec 2000 (ObsID 50804-01-14-00). There are 50 ObsID during this period, out of which 2 were not useful; during ObsID 50100-01-01-05 the Crab pulsar was completely occulted by the Earth ($\text{ELV} < 0^\circ$, which is the instantaneous angle between the Earth’s limb and the astronomical source); and ObsID 50099-01-05-00F was obtained on 11 Sept 2000, during the week when there were up to 1° errors in the spacecraft attitude. Six of the remaining 48 ObsIDs have more than 10% data gaps in them, but they have sufficient useful data for our purpose.

¹<http://www.jb.man.ac.uk/pulsar/crab.html>

²heasarc.gsfc.nasa.gov/docs/xte/data_analysis.html

Thus the Crab pulsar is under sampled (from the timing point of view) for most of the one year duration under consideration, except for three brief periods of well sampled data, one at the very beginning of the pre glitch duration, one just after the glitch, and one at the very end of the observations used in this work.

In fact the pre and post glitch duration were chosen based partly on the availability of closely spaced (frequently observed) data. The other reason was for the data to be sufficiently isolated in time from the previous and the next Crab pulsar glitches, so that the timing analysis is not corrupted by their residual effects. The previous Crab pulsar glitch (a small glitch) occurred at $\approx 00:29$ UTC on 1 Oct 1999, and the next glitch (a large one) occurred at $\approx 01:44$ UTC on 24 Jun 2001 (Espinoza et al. 2011); the very small glitch at $\approx 18:00$ UTC on 17 Sept 2000 is ignored because the data of this work is not sensitive to it. The first observation of this work is 78 days after the previous glitch, which is several times the longest of the short decay timescales for the Crab pulsar (Lyne et al. 2000; Wong et al. 2001; Wang et al. 2012), so one expects that the pre glitch timing solution in this work is not corrupted by the decay phenomenon of the previous glitch. The last observation of this work is six months before the next big Crab pulsar glitch.

3. Data Processing

All data used in this work have been acquired in the **Event List** mode (operating modes E_8us_256_DX0F, E_8us_256_DX1F, etc.), in which the photon arrival times have accuracy $\approx 7.6 \mu\text{sec}$ (the best possible for HEXTE), and also the highest energy resolution (256 channels in the energy range 0 to 250 keV); see “Reduction and Analysis of HEXTE data” on the RXTE website³. Throughout this analysis, data of each cluster are analyzed separately.

The first step in data processing is the creation of the so called Good Time Intervals (GTI), which are time duration identifying the useful data, not corrupted by instrumental and extraneous factors. The GTI that account for system provided checks are created by the tool **maketime** using the fil-

ter file available in the directory STDPROD, and using the screening criterion (1) $\text{ELV} > 10^\circ$, (2) the difference between the source position and the pointing of the satellite (OFFSET) $< 0.02^\circ$, (3) the time since the peak of the last South Atlantic Anomaly passage (TIME_SINCE_SAA) > 30 min or $\text{TIME_SINCE_SAA} < 0$ min.

3.1. Standard Processing of HEXTE Data

The next step is to create additional GTI based on the light curves of the observation; for example, abrupt changes of large magnitude in photon count rates should be excluded from the analysis.

For that, each data file for each cluster is processed by the tool **hxtback** to separate the data pertaining to source and sky background regions; for timing analysis only the source data are used. Then light curves are obtained using the tool **se-
extract**, screening the data using the GTI available in each file, as well as the GTI file created in the previous section. The light curves are binned at the telemetry interval DELTAT (16 sec), and photons are selected from energy channels 15 to 240 keV. The light curves are corrected for dead time using the tool **hxtdead**, using the appropriate house keeping file. Although all four detectors are chosen for both clusters while running the tools, the third detector of cluster 1 lost ability to assign energy information to a photon after 6 March 1996; photons of this detector fall in the first two energy channels irrespective of their actual energy. Therefore our choice of 15 to 240 keV energy range essentially filters out photons from this detector, even though they have valid arrival time information; see “The XTE Technical Appendix” on RXTE website⁴.

Light curves for both clusters are plotted, and the range of count rates, within which the data appears good, are chosen. These light curves and count rate limits are used to create a second set of GTI files, one for each cluster, using the tool **maketime**. These GTI are then merged with the earlier GTI, using the tool **mgtime** with the AND option, to yield the final GTI, which are then used to filter the individual data files, using the tool **fselect**. By this stage, one has screened the data for all system provided checks, as well as for user provided count rate limits. Finally, the pho-

³heasarc.gsfc.nasa.gov/docs/xte/recipes/cook_book.html

⁴heasarc.gsfc.nasa.gov/docs/xte/appendix_f.html

ton arrival times are referred to the solar system barycenter using the tool **faxbary**, using the orbit file for the given ObsID, and the Crab pulsar’s coordinates (83.6332208° for right ascension and 22.0144611° for declination, for the epoch J2000, (McNamara 1971), taken from the online pulsar catalog of ATNF⁵).

3.2. Obtaining the Period of Crab Pulsar

The next step is to obtain the best period of the Crab pulsar for each data file of each cluster. The fundamental frequency in the power spectrum of the data gives the first approximation to the period, which is obtained using the tool **powspec**, with bin size 0.67 ms and data length $2^{20} = 1048576$ bins for most files, but half or quarter of that for shorter files. This is done for each data file of each cluster, not only to check for consistency of the period among all files of a single ObsID, but also to check the health of the data. The second approximation to the period is obtained by folding the data over a range of 600 periods centered on the first approximation period, and searching for the maximum χ^2 , using the tool **efsearch**, with an increment of 10^{-8} sec in period, and zero period derivative. The third approximation to the period is obtained by doing a finer search centered on the second approximation period, using an increment of 0.2×10^{-8} sec in period, and a nominal period derivative of 420×10^{-15} sec per sec (explained later), over a range of 128 periods. A Gaussian is fit to the χ^2 as a function of period, to obtain the centroid. The final period is obtained by folding the earlier and later portions of the data at the third approximation period, then cross correlating the two integrated profiles, then measuring the shift (if at all) versus time between the two profiles. Folding is done using the tool **efold**, while cross correlation is done using independently developed software. The accuracy of the final period was typically 7 nano sec; for ObsID with long duration observations it could be as small as fraction of a nano sec.

3.3. Obtaining the Epoch of the Main peak of Crab Pulsar

The next step is to combine data files of each ObsID to get the integrated profile of the Crab pulsar separately for each cluster, with a resolution of 128 bins per period, using the best period of the epoch, and a nominal period derivative of 420×10^{-15} sec per sec, that is obtained by fitting the periods versus epochs for the 48 ObsIDs; this value is also consistent with the mean period derivative of the Crab pulsar for the duration Dec 1999 to Dec 2000, as estimated from radio data, given in the Jodrell monthly ephemeris. The zero phase of the integrated profile is set to the arrival time of the first valid photon in the data, after conversion to MJD by adding the MJDREF available in the data files. For validity of this procedure, it must be ensured that the keyword RADECSYS in the barycenter corrected data files is set to FK5, the keyword TIMEZERO is set to 0, and the keyword CLOCKAPP is set to T; see “A Time Tutorial” in “The ABC of XTE” guide, and also “RXTE Absolute Timing Accuracy” on RXTE website⁶.

The final step is to obtain the epoch of arrival of the peak of the main pulse of Crab pulsar, which is taken as the fiducial point in its integrated profile. For this the epoch of the zero phase of the integrated profile (described above) should be added to the position of the peak of the main pulse. This position is found by three independent means, as done in (Rots et al. 2006) but with some difference – (1) fitting a Gaussian to the main peak data, (2), fitting a Lorentzian to the main peak data, and (3) finding the first moment of the main peak data higher than 80% of the peak value. The first difference with (Rots et al. 2006) is that they fit a parabola instead of a Gaussian in method (1). The second difference is that they have 200, 400 and 800 bins in the integrated profile for the three methods, respectively, whereas the number of bins in this work are 128 for all three methods, because several ObsID do not have sufficient exposure to obtain sufficient signal to noise ratio with higher number of bins. The disadvantage of having lower number of bins in the integrated profile is that one has to be cautious while fitting the Gaussian and the Lorentzian; one has to choose as much of

⁵www.atnf.csiro.au/research/pulsar/psrcat/

⁶heasarc.gsfc.nasa.gov/docs/xte/abc/time.html

the main peak data as possible, to maximize the sensitivity of the fit, but should not include the asymmetric parts of the peak in its wings. This fitting is done for each cluster for each ObsID. All three methods give consistent timing results for the Crab pulsar glitch of July 2000. The typical accuracy of the fit is ≈ 1 milli period. Figure 1 shows the integrated profile of the Crab pulsar for ObsID 40090-01-01-00 for the combined data of both clusters.

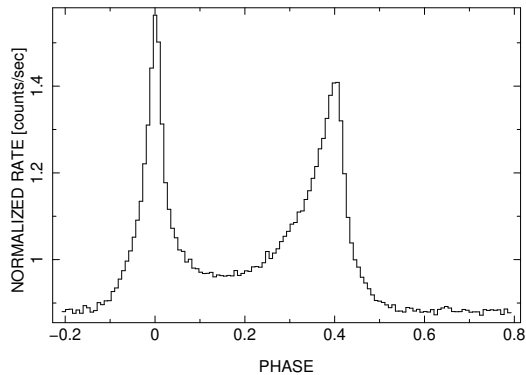


Fig. 1.— Integrated profile of Crab pulsar obtained by combining data of ObsID 40090-01-01-00 from both clusters. The epoch of the peak of the main pulse of cluster 0 data is used as reference phase for the tool **efold**, and data is folded at the period of this epoch (0.0335046788 sec). The average counts per sec (used to normalize the ordinate) is 176.477783.

4. Phase Coherent Timing Solution for the July 2000 Glitch

The timing solution for Crab pulsar presented in this work was obtained using the Gaussian fitting method described earlier, with three variations of epoch of arrival of the peak of the main pulse (henceforth referred to as pulse arrival epoch) – (1) epochs from data of cluster 0 only, (2) epochs from data of both clusters, but separately, and (3) epochs from combined data of both clusters. Methods (1) and (3) both have 48 epochs, while method (2) has twice the number. The epochs from method (3) are expected to be the most reliable due to enhanced number of photons in the integrated profile by the average factor 1.75 (cluster 1 gathers 25% less photons due to excluding detector 3). All three methods give consis-

tently similar results. The results presented in this work are derived using method (3). As mentioned earlier, timing solutions obtained using method (3) along with fitting a Lorentzian, and finding the first moment, all give results similar to those presented in Table 2 in this work. In addition, compared to the Gaussian fit method, the first moment method gave a mean departure of 1 ± 2 milli periods for the 48 epochs; for the Lorentzian method the mean departure was 0.3 ± 0.4 milli periods. Thus it is concluded that pulse arrival epochs are consistent among the three peak finding methods.

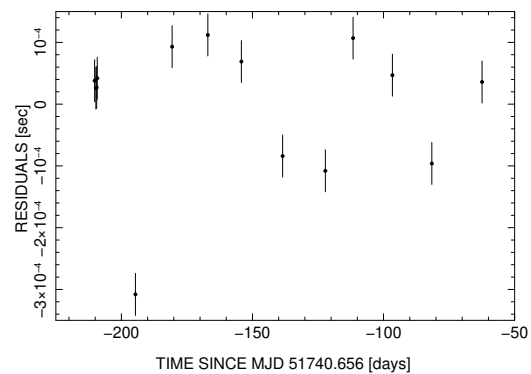


Fig. 2.— Result of using TEMPO2 on the 14 pre glitch pulse arrival epochs, fitting for ν , $\dot{\nu}$ and $\ddot{\nu}$, using the epoch of the first data at -210.221 (MJD 51530.4349129857) as the reference epoch for phase zero in TEMPO2; the results are given in Table 1. The origin of the abscissa is at the epoch of the glitch (MJD 51740.656). Note the four closely spaced epochs at the start of the data, and the lack of any observation for two months prior to the glitch.

Table 1: TEMPO2 best fit parameters to the pre glitch data of Figure 2. ν is the rotation frequency of the Crab pulsar at the epoch MJD 51530.4349129857, which is the first epoch in our data; $\dot{\nu}$ and $\ddot{\nu}$ are the first and second time derivatives of ν , respectively, at the same epoch. The errors in brackets are in the last digit of each result.

Parameter	Value
ν (Hz)	29.846592902(2)
$\dot{\nu}$ (10^{-10} s $^{-2}$)	-3.745962(8)
$\ddot{\nu}$ (10^{-20} s $^{-3}$)	0.94(1)

Figure 2 shows the result of using TEMPO2

(Hobbs et al. 2006) on the 14 pre glitch pulse arrival epochs. In the absence of glitches and timing noise, pulsars obey a simple slowdown model that is adequately represented, at least for short duration of several months, by three parameters – rotation frequency ν , its time derivative $\dot{\nu}$ and its second derivative $\ddot{\nu}$; see Equation 1 of (Espinoza et al. 2011). The three fitted parameters are shown in Table 1, and are consistent with the interpolated values from the Jodrell monthly ephemeris for the Crab pulsar for that epoch. The formal one standard deviation error on the pulse arrival epoch in Figure 2 is typically 0.87 milli periods. An independent estimate of the error is obtained by the difference in pulse arrival epochs for clusters 0 and 1 for the same ObsID. Often these differ by ≈ 16 sec or a few multiples of it, but on rare occasions can differ by hours. Ideally these relatively short duration differences should be equivalent to almost integer number of pulse cycles, since the estimated period of rotation of the Crab pulsar would be very accurate for closely spaced epochs; the departure from integer values will give us an idea of the errors involved in pulse arrival epochs in Figure 2. The mean value of the departure from integer number of cycles turns out to be ≈ 1.0 milli period. Therefore all error bars in Figure 2 are set to one milli period. The rms residual of the 14 pre glitch arrival times after the TEMPO2 fit is 3.2 milli periods.

TEMPO2 is used with the parameters of Table 1 as constant input (i.e., without any fitting) for the 34 post glitch pulse arrival epochs; the results are shown in Figure 3. These post glitch residuals $\Delta\phi$ (in sec) are fit to a modified version of the glitch model of (Shemar & Lyne 1996),

$$\begin{aligned} \Delta\phi &= -\frac{1}{\nu_0} \int_{\epsilon}^t dt \left[\Delta\nu_p + \Delta\dot{\nu}_p t + \Delta\nu_n \exp\left(-\frac{t}{\tau_d}\right) \right] \\ &\approx -\Delta\phi_0 - \frac{\Delta\nu_p}{\nu_0} t - \frac{\Delta\dot{\nu}_p}{\nu_0} \frac{t^2}{2} \\ &\quad - \frac{\tau_d \Delta\nu_n}{\nu_0} \left(1 - \exp\left(-\frac{t}{\tau_d}\right) \right), \end{aligned} \quad (1)$$

where t is the time elapsed since the glitch epoch (in seconds), ν_0 is the rotation frequency of the Crab pulsar at the epoch of the glitch (in Hz), $\Delta\nu_p$ and $\Delta\nu_n$ are the permanent and exponentially decaying parts of the step change in rota-

tion frequency at the epoch of the glitch, $\Delta\dot{\nu}_p$ is the permanent step change in the time derivative of the rotation frequency, and τ_d is the decay time scale (in sec) of the step frequency change. The parameter $\Delta\phi_0$ accounts for any uncertainty ϵ in the epoch of the glitch, which is assumed to be much smaller than τ_d . The equation above differs from Equation 1 of (Shemar & Lyne 1996) in having a single exponential only; as mentioned in their paper, only occasionally one requires more than one transient component, and the decay times of these additional transients are typically hundreds of days. The negative sign in Equation 1 accounts for the fact that the phase residuals after a glitch increase in the negative direction for a positive step change in rotation frequency (Shemar & Lyne 1996). Table 2 gives the minimum χ^2 fit values of the parameters in Equation 1. The rms residual of the 34 post glitch arrival times after the fit is 8.6 milli periods.

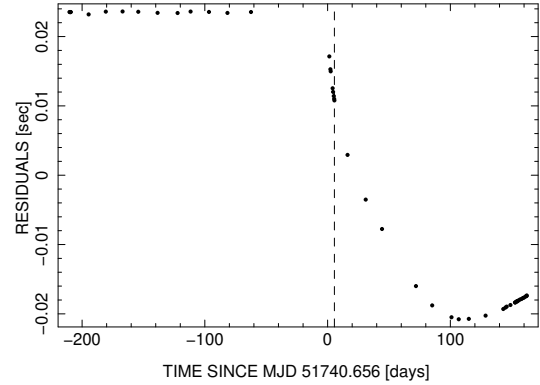


Fig. 3.— Result of using TEMPO2 on the 34 post glitch pulse arrival epochs, using the values of Table 1 as input parameters and without fitting. The origin of the abscissa is at the epoch of the glitch (MJD 51740.656). The vertical dashed line is at epoch after which one phase cycle was subtracted for all subsequent epochs, using the command PHASE -1 in the input file to TEMPO2. Note the clusters of closely spaced epochs, one just after the glitch epoch, and the other at the end of the data.

The epoch of the glitch is set to the published value of MJD 51740.656, since our data is unable to verify this number. (Espinoza et al. 2011) obtain this by using trial glitch epochs as reference epochs in TEMPO2 for the pre and post glitch timing solutions, then comparing the two solutions

Table 2: Minimum χ^2 parameters obtained by fitting Equation 1 to the post glitch data of Figure 3.

Parameter	Value
$\Delta\phi_0$ (ms)	3.3 ± 0.5
$\Delta\nu_p$ (10^{-6} Hz)	0.180 ± 0.003
$\Delta\dot{\nu}_p$ (10^{-13} s $^{-2}$)	-0.350 ± 0.006
$\Delta\nu_n$ (10^{-6} Hz)	0.71 ± 0.08
τ_d (days)	4.7 ± 0.5

for a match in phase at the reference epoch (glitch epoch). This is not possible in this work because of under sampling of data; the one and only pre glitch solution available (Table 1) was with the reference epoch used, because close to that the data was well sampled. An alternate method of formulating the parameter $\Delta\phi_0$ is to take the integral in Equation 1 from the limits 0 to $t - \epsilon$, instead of from ϵ to t . It can be shown that the two methods are equivalent as long as $\epsilon/\tau_d \ll 1$, and the derived parameters $\Delta\nu_p$, $\Delta\dot{\nu}_p$ and $\Delta\nu_n$ have the relative orders of magnitude as derived in Table 2.

The total step change in rotation frequency at the glitch, as a fraction of the pre glitch frequency, is $(\Delta\nu_p + \Delta\nu_n)/\nu_0 = (30 \pm 3) \times 10^{-9}$, which is not too different from the value of $(25.1 \pm 0.3) \times 10^{-9}$ published by (Espinoza et al. 2011). The actual step change of $\Delta\nu_p + \Delta\nu_n \approx 0.89 \pm 0.08$ μ Hz compares well with the top panel of Figure 5 of (Espinoza et al. 2011). The fraction of frequency recovery Q is $0.71/(0.71 + 0.18) \approx 0.80 \pm 0.11$, which is very high, as evident from Figure 5 of (Espinoza et al. 2011), although the decay of frequency in their figure (top panel) does not appear to be entirely exponential, most probably due to the very small glitch that has been ignored in this work.

The total step in frequency derivative at the glitch as a fraction of the pre glitch frequency derivative is $(\Delta\dot{\nu}_p - \Delta\nu_n/(\tau * 86400))/\dot{\nu}_0 = (4.8 \pm 0.6) \times 10^{-3}$, which is also not too different from the value of $(2.9 \pm 0.1) \times 10^{-3}$ of (Espinoza et al. 2011). The fraction of recovery of the frequency derivative is $-17.48/(-17.48 - 0.35) \approx 0.98 \pm 0.16$, which is consistent with Figure 5 of (Espinoza et al. 2011). However, the step change in $\dot{\nu}_0 \approx (-18 \pm 2) \times 10^{-13}$ estimated here is inconsistent with the bottom panel of Figure 5 of (Espinoza et al. 2011), in which it is more like $\approx -5 \times 10^{-13}$.

However, the value expected from their work is $\approx 2.9 \times 10^{-3} \times -3.744255 \times 10^{-10} \approx -11 \times 10^{-13}$, which is in between the above two numbers.

(Espinoza et al. 2011) do not quote a value for the decay time scale τ_d for this glitch. By expanding and gridding their Figure 5, and reading off values of the peak and the first decay point, one can obtain an approximate value for τ_d . This turns out to be $\approx 13 \pm 3$ days, for the decay of both the frequency and its derivative (top and bottom panels respectively of that figure). The number derived in this work, $\tau_d = 4.7 \pm 0.5$ days, is a factor of ≈ 2.8 smaller, although it is in the right range of decay time scales for Crab pulsar (Lyne et al. 2000). If it turns out that the correct value of τ_d is indeed ≈ 13 days, then the reason for the factor of 2.8 underestimate in this work is most probably on account of lack of observations very close to the glitch epoch, to which the estimate of τ_d is very sensitive.

5. Discussion

In section 4 we concluded that the hard xray timing of the Crab pulsar glitch of 15 July 2000, using HEXTE/RXTE data, is consistent with the results obtained at radio frequencies by the Jodrell Bank observatory. This is, to the best of our knowledge, the first time that a glitch of the Crab pulsar has been analyzed using xray data, resulting in what can be considered to be the closest to absolute timing of the Crab pulsar at hard xray energies.

(Rots et al. 2006) found that the main peak of the xray pulse profile of the Crab pulsar (the peak at phase 0 in Figure 1) leads the main peak of the radio pulse profile (just after the radio precursor; see Figure 6a of (Kuiper et al. 2003)) by 344 ± 40 μ sec. Figure 4 shows the result of fitting the data of Figure 3 combined with the Jodrell data at radio frequencies, obtained from their monthly ephemeris. It shows the combined pre and post glitch residuals after subtracting the pre and post glitch models, respectively. The pre glitch model is given in Table 1. The post glitch model is obtained by including additionally in Equation 1, permanent step changes in the second and third time derivatives of the rotation frequency, $\Delta\ddot{\nu}_p$ and $\Delta\ddot{\nu}_n$, respectively. This solution gave the lowest rms residual of 3.2 milli periods for the 34

post glitch arrival times; the values of the rest of the parameters obtained in this fit are consistent with those in Table 2. The mean pre glitch separation of the Jodrell data with respect to the xray data is $411 \pm 167 \mu\text{sec}$. Although this result has ≈ 4.2 times larger error than that quoted by (Rots et al. 2006), it is consistent with their result, and also with the results of others (Kuiper et al. 2003; Carrillo et al. 2012). The post glitch differences with Jodrell data are difficult to analyze, due to the baseline varying in a quasi periodic manner. However, after accounting for these variations, the last three post glitch Jodrell data certainly support the above number.

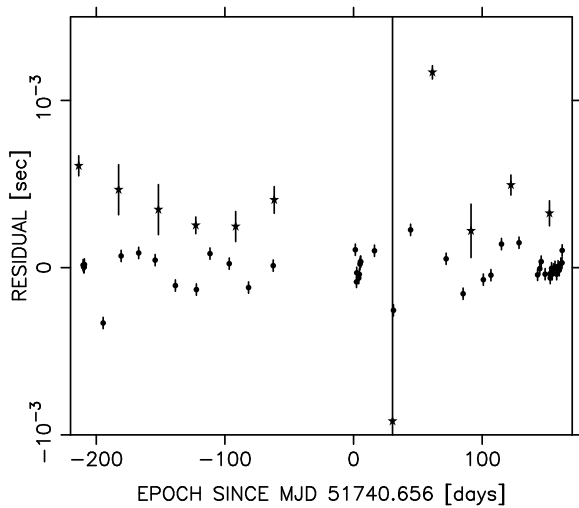


Fig. 4.— Pre and post glitch xray residuals (this work, dots; see text for the corresponding models) along with eleven radio residuals from Jodrell Bank data (stars), which lie consistently above xray residuals, except for the residual of 15 Aug 2000, which has a very large error bar (4 ms).

Several properties of the Crab pulsar can be studied as a function of pre and post glitch epochs. Three parameters were plotted as a function of epoch – (1) The separation of the two peaks in the Crab pulsar’s integrated profile, (2) the ratio of their peaks, and (3) integrated energy in the pulse profile. The first two showed no variation worth reporting (see also (Rots et al. 2006)). Figure 5 shows the dead time corrected photon count variation of the Crab pulsar as a function of epoch.

Each point in Figure 5 is obtained by first estimating the average off pulse counts in the in-

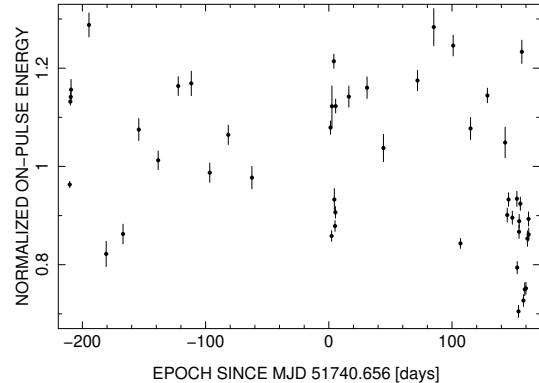


Fig. 5.— Normalized and dead time corrected on pulse energy of Crab pulsar during the year 2000.

tegrated profile, then subtracting it from the on pulse counts before integrating them, then dividing the result by the average off pulse counts; this is done for every DELTAT (16 sec) of data for each ObsID. Off pulse counts are obtained by integrating in the phase range 0.61 to 0.79 in Figure 1; the rest of phase range represents the on pulse. Although this procedure will exclude any small off pulse emission from the Crab pulsar (Tennant et al. 2001), it has the advantage of correcting for dead time, which is not available for Barycenter corrected data, and also for data that has been filtered in energy range, which is the situation with our data; see “The XTE Technical Appendix” on RXTE website⁷. Finally all 48 energies are normalized by their mean value, which lies at the value 1.0 in Figure 5. The assumption made here is that dead time correction is, to a large order of accuracy, the same for the on and off pulse phases of a pulsar, even for bright pulsars such as the Crab. Dead time is the duration immediately after the arrival of an xray photon or high energy particle, during which the HEXTE detectors are unable to process any more photons. For the HEXTE detector there are two sources of dead time. One is due to the arrival of an xray photon, after which the HEXTE detectors are “dead” for 16 to 30 μsec . The much larger effect is due to arrival of high energy particles, after which the detectors are dead for 2500 μsec ; these are known as XULD events. Even for a luminous pulsar such

⁷heasarc.gsfc.nasa.gov/docs/xte/appendix_f.html

as the Crab and its nebula, the normal photon count rate is typically < 400 photons per sec per cluster, while the normal XULD event rate is typically 150 particles per sec per detector (there are 4 detectors per cluster). Taking the mid value of $23 \mu\text{sec}$, it can be easily seen that the ratio of the photon to XULD contribution to the dead time is $\leq 0.6\%$. Since the XULD event rate is the same for on and off pulse regions, the above method of dead time correction is justified. If required, more refined dead time correction can be done by using the integrated pulse profile of the pulsar.

In Figure 5, the standard deviation of the spread in values is $\approx 16\%$ of the mean value; the corresponding spread in the uncorrected fluxes is $\approx 49\%$ of the mean value. This technique of dead time correction for pulsars significantly improves the precision of the estimate of integrated xray flux, and may therefore prove useful to find out if the Crab pulsar xray flux varies on time scales of decades; for the crab nebula this has already been observed at several xray energies (see (Wilson-Hodge et al. 2011) and references therein).

In Figure 5 there is no strong evidence for the xray flux of the Crab pulsar to be affected by the glitch. The mean pre and post glitch xray fluxes are 1.06 and 0.98, respectively, while the standard error on these means is 0.03. The mean xray fluxes differ by 0.08 ± 0.04 , which can not be considered a strong result. Moreover, this decrease appears to be mainly due to the data well after the glitch in Figure 5, making it less likely to be related to the glitch itself. One instrumental feature that can simulate such a result is a variation of the average off pulse counts as function of epoch in Figure 5; however this does not appear to be the case. Although this can not be considered a strong result, it may be interesting to speculate on the possible causes of glitch related xray flux variations in rotation powered pulsars. Such studies have not been done so far. Although glitch related xray flux enhancements have been reported in some Magnetars (see (Espinoza et al. 2011) and references therein), it is generally believed that in Magnetars and AXPs, glitches are not always associated with xray flux variations (Dib et al. 2008). For the Crab pulsar glitch under consideration here, the post glitch permanent changes in rotation frequency $\Delta\nu_p$ and its derivative $\Delta\dot{\nu}_p$ can contribute

at most to a fractional increase of $\approx 0.01\%$ in the post glitch xray flux, while Figure 5 shows a decrease of 8%; so simple energy loss rate of the Crab pulsar may not be the explanation. The glitch model of (Ruderman 2009) provides a causal connection between a glitch in a rotation powered pulsar and changes in its surface magnetic field. In this model, a glitch is caused by excessive stresses in the neutron star crust, that are built up by super fluid vortices moving outwards due to the spin down of the neutron star, dragging with them magnetic flux tubes. The crust cracks at the instant of the glitch, and then adjusts itself to a new configuration, leading to a corresponding reconfiguration of the surface magnetic field, presumably both in terms of its field strength as well as in terms of its field line structure (curvature of field lines, direction of the opening bundle of field lines at the surface, presence of higher magnetic multipoles, etc). There are several quantitative uncertainties in the predictions from this model. However it may be worth exploring if a small change in surface magnetic field structure of the Crab pulsar can lead to a non-linearly large change (decrease in the present case, but maybe an increase in other glitches) in the post glitch xray flux.

It is well known that the dispersion measure of the Crab pulsar varies due to radio propagation within the Crab nebula (Lyne et al. 1993), and that the radio pulses suffer significant and variable refractive and scattering effects within the Crab nebula (see (Backer et al. 2000) and references therein). Such effects can cause errors in the arrival times of the radio pulses, with consequent errors on the derived glitch parameters. The above interstellar effects are frequency dependent, and are absent for pulses at xray energies. The consistency between the radio and hard xray timing results of this work imply that the effect of radio pulse propagating through the Crab nebula has not been significant during the glitch of July 2000.

Glitches are one of the two timing irregularities observed in rotation powered pulsars, the other being timing noise, which manifests observationally as random wandering of timing residuals. It is currently believed that timing noise is due to instabilities in the pulsar magnetosphere (Lyne et al. 2010); see also (Arons 2009) and references therein for a possible theoretical explana-

tion in terms of magnetic reconnection. Now, the radio and xray emitting regions in the Crab pulsar's magnetosphere are supposed to be identical (the outer gaps), except for the radio precursor, which is supposed to arise in the polar gap, while for other rotation powered pulsars (eg. Vela) the radio and xray emitting regions are supposed to be different; see (Harding 2009) and references therein. Therefore simultaneous radio and xray studies of timing noise in the Crab pulsar should show similar timing noise properties (rms residuals, time scales of wandering, etc), but probably not in Vela like pulsars.

Glitches, on the other hand, are supposed to be due to the steady differential spin down of the super fluid core and outer crust of the neutron star; see (Ruderman 2009) and references therein. At the instant of the glitch, the outer crust speeds up, thereby also speeding up the pulse emitting regions in the magnetosphere, which are firmly anchored into the crust by means of the magnetic field. Simultaneous timing observations of pulsar glitches at radio and xray wavelengths can probably be used to find out if the emission regions at different energies are anchored equally firmly onto the surface of the neutron star. For example in the case of the Crab pulsar one would expect the glitch behavior to be almost identical, while for the Vela like pulsars one may or may not notice differences.

I thank the anonymous referee for detailed comments to improve this manuscript. This research made use of data obtained from the High Energy Astrophysics Science Archive Research Center Online Service, provided by the NASA-Goddard Space Flight Center.

Facilities: RXTE (HEXTE).

REFERENCES

- Arons, J. 2009, in *Neutron Stars and Pulsars*, Ed. W. Becker, Astrophysics and Space Science Library, Springer, 373
- Backer, D. C. and Hellings, R. W. 1986, *ARA&A*, 24, 537
- Backer, D. C., Wong, T. and Valanju, J. 2000, *ApJ*, 543, 740
- Baym G., Pethick C., Pines D., Ruderman M., 1969, *Nature*, 224, 872
- Martin-Carrillo, A., Kirsch, M. G. F., Caballero, I. et al 2012, *A&A*, 545, A126
- Dib, R., Kaspi, V. M., Gavril, F. P. 2008, *ApJ*, 673, 1044
- Espinoza, C. M., Lyne, A. G., Stappers, B. W., and Kramer, M. 2011, *MNRAS*, 414, 1679
- Harding, A. K. 2009, in *Neutron Stars and Pulsars*, Ed. W. Becker, Astrophysics and Space Science Library, Springer, 521
- Hobbs, G. B., Edwards, R.T. and Manchester, R. N. 2006, *MNRAS*, 369, 655
- Kuiper, L., Hermsen, W., Walter, R., et al 2003, *A&A*, 411, L31
- Lyne, A. G., Pritchard, R. S. and Graham Smith, F. 1993, *MNRAS*, 265, 1003
- Lyne, A. G., Shemar, S. L., and Graham Smith, F. 2000, *MNRAS*, 315, 534
- Lyne, A. G., and Graham Smith, F. 2006, *Pulsar Astronomy*, Cambridge Astrophysics
- Lyne, A. G., Hobbs, G. B., Kramer, M. et al 2010, *Sci*, 329, 408
- Lyne, A. G., Jordan, C. A., Graham Smith, F. et al 2015, *MNRAS*, 446, 857
- Manchester, R. N. and Taylor, J. H. 1977, *Pulsars*, W. H. Freeman
- McNamara, B. J. 1971, *PASP*, 83, 491
- Rothschild, R. E., Blanco, P. R., Gruber, D. E., Heindel, W. A., MacDonald, D. R., Marsden, D. C., Pelling, M. R. and Wayne, L. R. 1998, *ApJ*, 496, 538
- Rots, A. H., Jahoda, K. and Lyne, A. G. 2004, *ApJ*, 605, L129
- Ruderman, M., Zhu, T. and Chen, K. 1998, *ApJ*, 492, 267
- Ruderman, M. 2009, in *Neutron Stars and Pulsars*, Ed. W. Becker, Astrophysics and Space Science Library, Springer, 353
- Shemar, S. L. and Lyne, A. G. 1996, *MNRAS*, 282, 677
- Tennant, A. F. Becker, W., Juda, M. et al 2001, *ApJ*, 554, L173

- Wilson-Hodge, C. A., Cherry, M. L., Case, G. L. et al
2011, ApJ, 727, L40
- Wang, J., Wang, N., Tong, H., Yuan, J. 2012, Ap&SS,
340, 307
- Wong, T., Backer, D. C. and Lyne, A. G. 2001, ApJ,
548, 447